J. Plasma Physics (2012), *vol.* 78, *part* 4, *pp.* 333–337. © Cambridge University Press 2012
doi:10.1017/S0022377811000614

Collimation of laser-driven energetic protons in a capillary

D.-P. CHEN (陈德鹏)[1], Y. YIN (银燕)[1], Z.-Y. GE (葛哲屹)[1], H. XU (徐涵)[2], H.-B. ZHUO (卓红斌)[1], Y.-Y. MA (马燕云)[1], F.-Q. SHAO (邵福球)[1], and C.-L. TIAN (田成林)[1]

[1]Department of Physics, National University of Defense Technology, Changsha 410073, China (yyin@nudt.edu.cn)
[2]National Laboratory of Parallel and Distributed Processing, National University of Defense Technology, Changsha 410073, China

(Received 20 September 2011; revised 13 December 2011; accepted 15 December 2011; first published online 6 January 2012)

Abstract. Energetic divergent proton beams can be generated in the interaction of ultra-intense laser pulses with solid-density foil targets via target normal sheath acceleration (TNSA). In this paper, a scheme using a capillary to reduce the proton beam divergence is proposed. By two-dimensional particle-in-cell (PIC) simulations, it is shown that strong transverse electric and magnetic fields rapidly grow at the inner surface of the capillary when the laser-driven hot electrons propagate through the target and into the capillary. The spontaneous magnetic field collimates the electron flow, and the ions dragged from the capillary wall by hot electrons neutralize the negative charge and thus restrain the transverse extension of the sheath field set up by electrons. The proton beam divergence, which is mainly determined by the accelerating sheath field, is therefore reduced by the transverse limitation of the sheath field in the capillary.

1. Introduction

In recent years, generation of energetic proton or ion beams is of great research interest because of potential applications in fast ignition of inertial confinement fusion [1], proton radiography [2], and cancer therapy [3], etc. Mechanisms to produce energetic protons include target normal sheath field acceleration (TNSA) [4], shock acceleration [5, 6], radiation pressure dominated ion acceleration (RPA) [7, 8], dual-peaked electrostatic-field acceleration [9], and so on.

When the laser is linearly polarized with an intensity not much higher than 10^{21} W/cm^2, and the solid-density target has a thickness from several micrometers to tens of micrometers, then the TNSA mechanism is dominant [10]. Since the laser pulse is not intense enough to pass through the target, it launches large amounts of hot electrons from the front surface. When these hot electrons propagate through the target and reach the back side of the target, they establish a strong sheath electric field which accelerates protons on the rear target surface. In a typical TNSA regime, energetic protons with energy from several to tens of MeV can be produced [10]. However, because of the deformation of the sheath field due to plasma expansion, the proton beam accelerated in the TNSA regime is inevitably divergent. Several types of tailored targets have been proposed to improve the collimation of the proton beam [11–14], from which the main idea is to improve the uniformity of the sheath electric field by tailoring the rear side of the target and then improving the beam quality. It is experimentally demonstrated that focused proton beams can be produced by using spherically shaped targets [13]. By using solid foils of limited transverse extent, the transverse refluxing of hot electrons can maintain a denser and more homogeneous sheath field around the target, resulting in increased maximum proton energies and reduced divergence [14]. Another novel method for enhancing the collimation of the proton beam is to use a microlens [15]. The proton beam propagates through a hollow cylinder side-irradiated by an intense subpicosecond laser pulse, and the triggered transient field on the inner wall of the cylinder focuses the proton beam and thus decreases the divergence [15].

In this paper, we propose a method to improve the collimation of laser-driven proton beam with a capillary. A capillary refers to a canal with the wall consisting of insulated material and vacuum in the center. The inner diameter varies from several tens of nanometers to micrometers. Capillaries with typical radius of 50–100 nm (nanocapillaries) can be used to guide the transmission of highly charged ions produced by an Electron Cyclotron Resonance (ECR) source [16]. Recently, S. Z. Wu et al. demonstrated that a low-density-core-high-density-cladding target can collimate energetic electrons driven by intense laser due to the spontaneous magnetic field induced on the inner surface [17]. H. B. Cai et al. analyzed in detail how the spontaneous magnetic field is induced [18]. Such a low-density-core-high-density-cladding target is very similar to a capillary. In this

https://doi.org/10.1017/S0022377811000614 Published online by Cambridge University Press

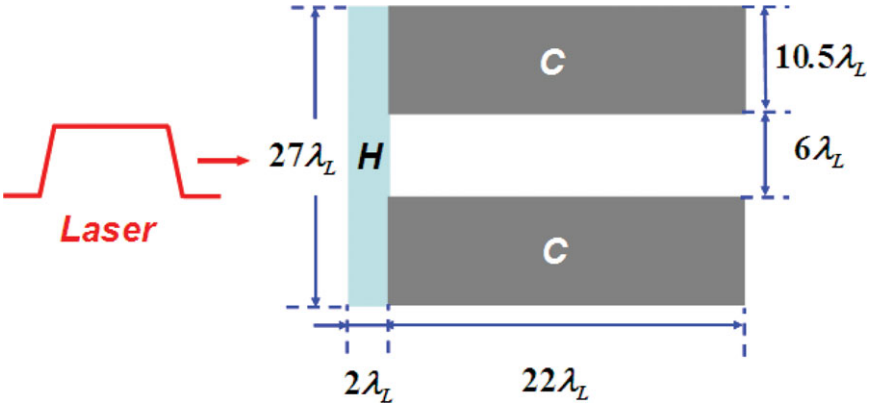


Figure 1. (Color online) A sketch of the simulated model.

paper, we investigate the guiding effect of a capillary on the propagation of energetic protons generated by the intense laser pulse. It is shown that the spontaneous magnetic field induced on the inner surface can effectively collimate the electron beam and restrain the transverse divergence of the sheath field. The protons undergo a more uniform electronic field and the proton beam divergence is decreased.

2. Simulation results and analysis

The simulation model is shown in Fig. 1. The two-dimensional simulation box is $30 \times 30\,\mu\text{m}^2$. A hydrogen plasma layer is placed from 1.5 to $3.5\,\mu$m in the x direction and from 1.5 to $28.5\,\mu$m in the y direction. The proton density is $n_i^{(H)} = 50n_c$, where $n_c = 1.1 \times 10^{21}/\text{cm}^3$. A hollow target is attached to the rear side of the hydrogen plasma. The wall of the capillary is composed of carbon plasmas with the carbon ion density $n_i^{(C)} = 100n_c$. The thickness of the wall is $10.5\,\mu$m, and the length is $22\,\mu$m. Absorption boundary conditions are employed in both x and y directions for both electromagnetic field and particles. The structure of the target is very similar to that of the low-density-core-high-density-cladding target which has been studied by H. B. Cai [18], but here the core of the capillary is vacuum. A linearly polarized laser with the wavelength $\lambda_L = 1\,\mu$m is incident from the left side along the x direction. The laser has a trapezoidal temporal profile. The intensity rises in $2T_L$ reaching the peak intensity of $I_L = 10^{21}\,\text{W/cm}^2$, keeps constant for $20T_L$, and then goes down to zero in $2T_L$. The transverse profile of the laser pulse is Gaussian with a full width at half maximum focal spot $\tau = 14.4\lambda_L$.

The intense laser pulse irradiates normally on the thin hydrogen plasma target. With the parameters here, the target is thick enough to shield the laser, and the main proton acceleration mechanism is TNSA. For comparison, the interaction under the same conditions but without the capillary is also simulated. The proton density evolution in the cases with and without a capillary are shown in Fig. 2. For the case with a capillary, shown in Fig. 2(a), energetic protons emerge from the rear side of the target. These protons enter and are transported in the capillary. With time, the proton beam is constricted in the transverse direction, and the proton front is squeezed to a line shape, as shown in Fig. 2(b). On the contrary, for the case without a capillary, shown in Figs. 2(c) and (d), the protons are quickly dispersed transversely. Clearly, the collimation of accelerated ions is improved by using a capillary. Figures 2(e) and (f) show the energy spectrum of accelerated protons in the region $y \in [12\,\mu\text{m}, 18\,\mu\text{m}]$ at $t = 40T_L$ and $80T_L$, respectively. It is seen that the maximum energy of protons in the case with a capillary is smaller than that in the case without a capillary, which indicates that the accelerating sheath field becomes weaker when a capillary is used.

The transverse restriction of protons in the capillary is related to the electric and magnetic fields stimulated in the capillary. Figure 3 shows the spatial distribution of the electron density, the ion density (including protons and carbon ions), the transverse electric field E_y, and the transverse magnetic field B_z at $t = 30T_L$. Figure 3(a) shows that laser-driven hot electrons enter the hollow core of the capillary and form a cloud of negative charge density in the capillary. The electrons not only set up a longitudinal sheath field accelerating protons, but also stimulate a transverse electric field E_y, as shown in Fig. 3(c). The transverse electric field points to the center of the capillary, focusing protons but defocusing electrons. When electrons are pushed laterally and enter the wall of the capillary, the negative charge can be quickly neutralized by the ions in the wall. As a result, E_y evanesces quickly into the wall over the skin depth. On the other hand, the accelerating sheath field is weakened, resulting in a smaller cutoff proton energy as shown in Figs. 2(e) and (f). Strong transverse magnetic field B_z is also stimulated at the inner surface of the capillary wall, as shown in Fig. 3(d). The hot electrons entering the wall stimulate the background return current, so there is a rapid change in the current flow velocity at the wall surface, which results in the generation of the strong magnetic field [18]. For electrons moving forward, the magnetic field provides a Lorentz force pointing to the center of the core, thus radially confining the

https://doi.org/10.1017/S0022377811000614 Published online by Cambridge University Press

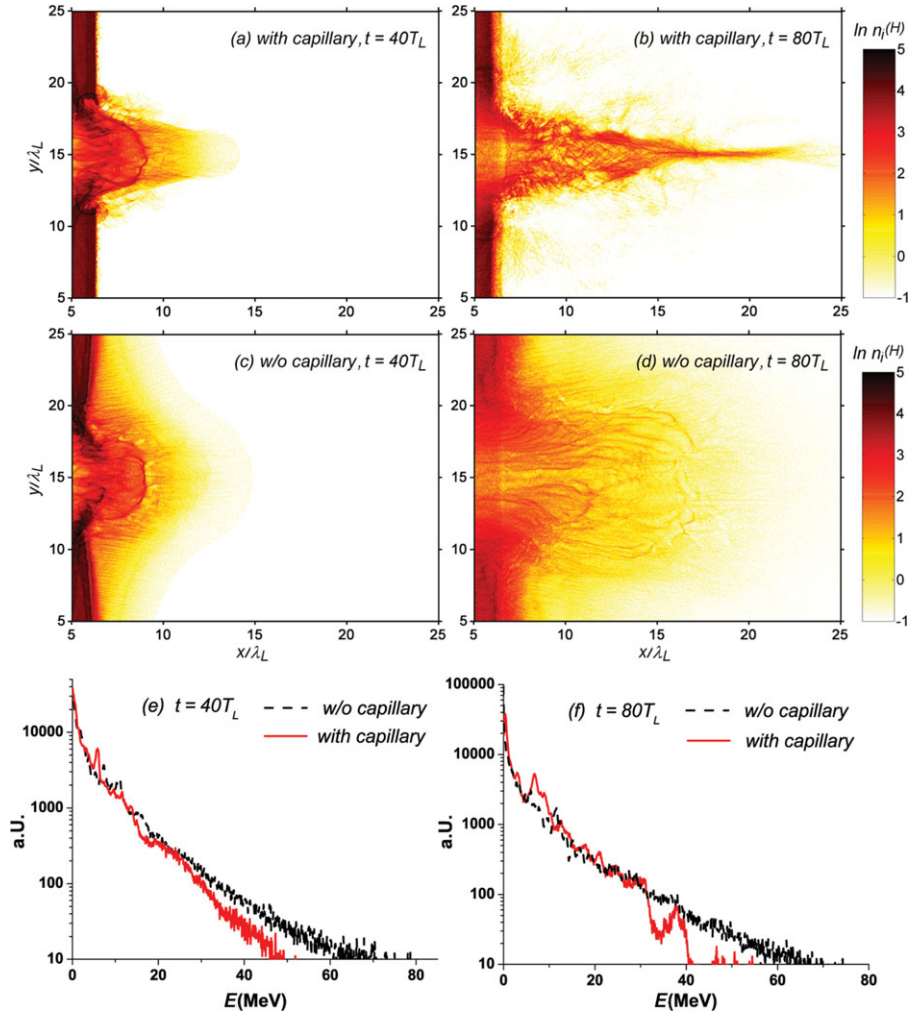


Figure 2. (Color online) Spatial density distribution of protons in logarithm scale at $t = 40T_L$ and $t = 80T_L$: (a) and (b) correspond to the case with a capillary; (c) and (d) correspond to the case without a capillary. The energy spectrum of accelerated protons in the region $y \in [12\,\mu\text{m}, 18\,\mu\text{m}]$: (e) at $t = 40T_L$; (f) at $t = 80T_L$.

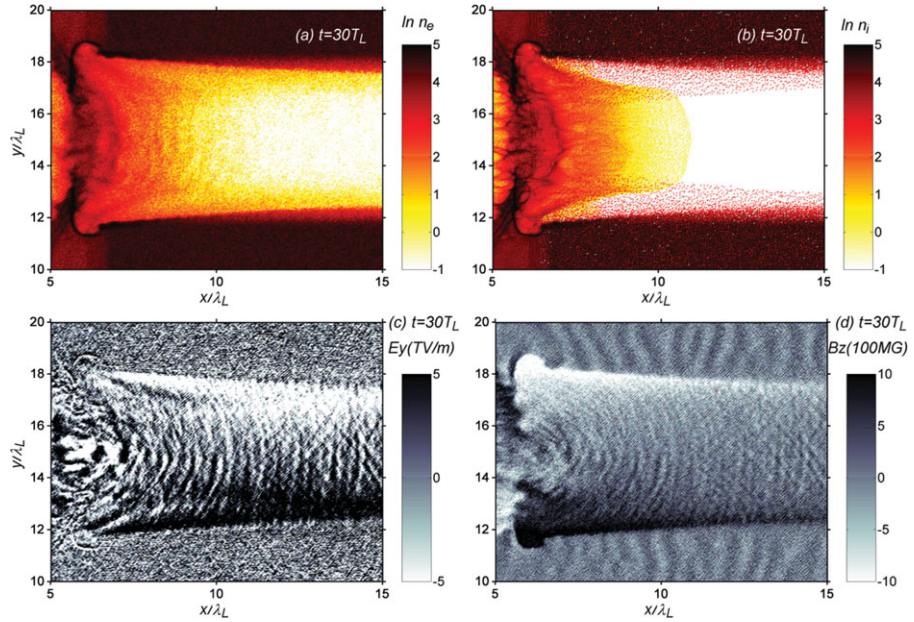


Figure 3. (Color online) The spatial distribution of the electron density (a), the ion (including protons and carbon ions) density (b), the transverse electric field E_y (c), and the transverse magnetic field B_z (d) at $t = 30T_L$.

https://doi.org/10.1017/S0022377811000614 Published online by Cambridge University Press

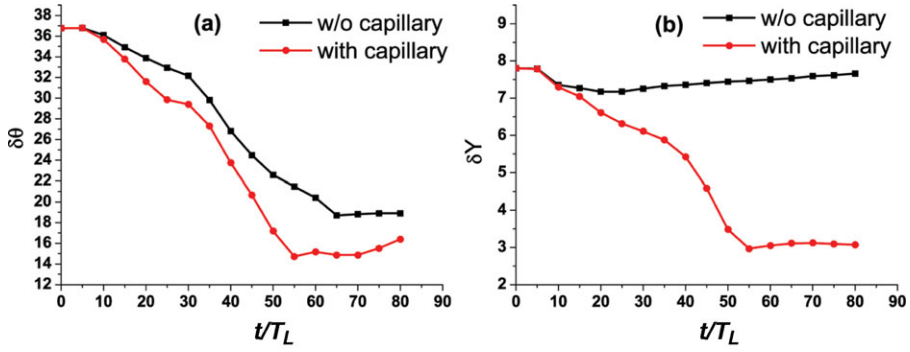


Figure 4. (Color online) The time evolution of the divergence angle $\delta\theta$ (a) and the radius δy (b) of the proton beam in the case with a capillary (black filled squares) and the case without a capillary (red filled circles).

electron flow. For protons, the magnetic field provides a scattering Lorentz force. The rotation radius of a charged particle in a magnetic field can be inferred from the dynamics equation as $r = mv/qB$, where m is the particle mass and q is the particle charge. So, the rotation radius of a proton is much larger than that of an electron. The scattering effect of protons is much smaller compared with the collimation effect of electrons. Due to the pushing effect of E_y and the collimation effect of B_z, most energetic electrons propagate along the inner surface of the capillary, as shown in Fig. 3(a). The sheath field built up by electrons is thus restricted in the capillary. Figure 3(b) shows the density distribution of all ions, including protons from the hydrogen foil and carbon ions from the wall of the capillary. Carbon ions are dragged from the wall of the capillary by energetic electrons, partially neutralizing negative charges and thus weakening the sheath field adjacent to the wall surface. The protons are accelerated in the restricted sheath field, exhibiting a transversely constricted density front.

For every proton moving forward ($v_x > 0$), the divergence angle $\theta = \arctan(v_y/v_x)$ is measured. The divergence angle of the proton beam can be defined as the variance of θ, and is denoted as $\delta\theta = \sqrt{\sum(\theta_i - \overline{\theta})^2/N}$, where N is the total number of protons moving forward and $\overline{\theta} = \sum\theta_i/N$. The collimation of the proton beam can be described quantitatively by $\delta\theta$. The radius of the proton beam can also be defined as $\delta y = \sqrt{\sum(y_i - \overline{y})^2/N}$, where the sum is over all protons moving forward and $\overline{y} = \sum y_i/N$. Figure 4 shows how $\delta\theta$ and δy change as functions of time for both the case with a capillary (black filled squares) and the case without a capillary (red filled circles). In both cases, the absolute value of the average divergence angle $|\overline{\theta}|$ is smaller than 0.3°, and the difference of $\overline{y}$ from the position of the capillary axis $y_{\mathrm{mid}} = 15\,\mu$m is negligible. In Fig. 4(a), it can be seen that $\delta\theta$ is always smaller in the case with a capillary than that in the case without a capillary. In Fig. 4(b), it can be seen that δy decreases rapidly in the case with a capillary, while the proton beam in the case without a capillary keeps a large radius. From Figs. 4(a) and (b), it can be seen that a narrow proton beam with low divergence is obtained by using a capillary.

In the above simulation, optimized laser and plasma parameters are chosen so that the hydrogen foil can reflect the laser pulse just before it breaks. If the laser pulse is strong enough to pass through the target and enter the capillary, the electromagnetic field of the laser will destroy the capillary wall, thus hazarding the divergence control of the proton beam.

3. Conclusion

In this paper, we propose a method to reduce the divergence of laser-accelerated proton beams by placing a capillary at the rear side of the laser-irradiated solid target. Using two-dimensional PIC simulation, it is shown that the sheath field set up by laser-driven electrons is restricted transversely in the capillary, and the strong magnetic field stimulated at the inner surface of the capillary wall can collimate the electron flow effectively. Protons, which are driven by electrons and are accelerated by the sheath field, are consequently collimated. Compared with the reference case without a capillary, both the divergence and radius of the proton beam propagating in the capillary are obviously reduced.

Acknowledgement

This work is supported by the National Science Foundation of China (Grant No. 11175255).

References

[1] Roth, M., Cowan, T. E., Key, M. H., et al. 2001 *Phys. Rev. Lett.* **86**, 436.

[2] Borghesi, M., Fuchs, J., Bulanov, S. V., Mackinnon, A. J., Patel, P. K. and Roth, M. 2006 *Fusion Sci. Technol.* **49**, 412.

[3] Bulanov, S. and Khoroshkov, V. 2002 *Plasma Phys. Rep.* **28**, 453.

[4] Wilks, S. C., Langdon, A. B., Cowan, T. E., Roth, M., Singh, M., Hatchett, S., Key, M. H., Pennington, D., MacKinnon, A., Snavely, R. A., et al. 2001 *Phys. Plasmas* **8**, 542.

[5] Zhang, X. M., Shen, B. F., Li, X. M., Jin, Z. Y., Wang, F. C. and Wen, M. 2007 *Phys. Plasmas* **14**, 123108.

https://doi.org/10.1017/S0022377811000614 Published online by Cambridge University Press

[6] Chen, M., Sheng, Z. M., Dong, Q. L., He, M. Q., Li, Y. T., Bari, M. A. and Zhang, J. 2007 *Phys. Plasmas* **14**, 053102.

[7] Yan, X. Q., Lin, C., Sheng, Z. M., Guo, Z. Y., Liu, B. C., Lu, Y. R., Fang, J. X. and Chen, J. E. 2008 *Phys. Rev. Lett*. **100**, 135003.

[8] Macchi, A., Veghini, S. and Pegoraro, F. 2009 *Phys. Rev. Lett*. **103**, 085003.

[9] Zhuo, H. B., Chen, Z. L., Yu, W., Sheng, Z. M., Yu, M. Y., Jin, Z. and Kodama, R. 2010 *Phys. Rev. Lett*. **105**, 065003.

[10] Passoni, M., Bertagna, L. and Zani, A. 2010 *New J. Phys.* **12**, 045012.

[11] Sonobe, R., Kawata, S., Miyazaki, S., Nakamura, M. and Kikuchi, T. 2005 *Phys. Plasmas* **12**, 073104.

[12] Okada, T., Andreev, A. A., Mikado, Y. and Okubo, K. 2006 *Phys. Rev*. E. **74**, 026401.

[13] Patel, P. K., Mackinnon, A. J., Key, M. H., Cowan, T. E., Foord, M. E., Allen, M., Price, D. F., Ruhl, H., Springer, P. T. and Stephens, R. 2003 *Phys. Rev. Lett*. **91**, 125004.

[14] Buffechoux, S., Psikal, J., Nakatsutsumi, M., Romagnani, L., Andreev, A., Zeil, K., Amin, M., Antici, P., Burris-Mog, T., Compant-La-Fontaine, A., et al. 2010 *Phys. Rev. Lett*. **105**, 015005.

[15] Toncian, T., Borghesi, M., Fuchs, J., d'Humières, E., Antici, P., Audebert, P., Brambrink, E., Cecchetti, C., Pipahl, A., Romagnani, L., et al., 2006 *Science* **312**, 410.

[16] Stolterfoht, N., Bremer, J.-H., Hoffmann, V., Hellhammer, R., Fink, D., Petrov, A. and Sulik, B. 2002 *Phys. Rev. Lett*. **88**, 133201.

[17] Wu, S. Z., Zhou, C. T. and Zhu, S. P. 2010. *Phys. Plasmas* **17**, 063103.

[18] Cai, H. B., Zhu, S. P., He, X. T., Wu, S. Z. and Chen, M. 2011 *Phys. Plasmas* **18**, 023106.

https://doi.org/10.1017/S0022377811000614 Published online by Cambridge University Press